11-15-2007

Wide-Angle Achromatic Prism Beam Steering for Infrared Countermeasure Applications

Philip J. Bos
Kent State University - Kent Campus, pbos@kent.edu

Henry Garcia

Vassili Sergan

Performance evaluation of a liquid-crystal-on-silicon spatial light modulator

Xinghua Wang, MEMBER SPIE
Bin Wang, MEMBER SPIE
Kent State University
Liquid Crystal Institute
Kent, Ohio 44242

John Pouch
Felix Miranda
NASA Glenn Research Center
Cleveland, Ohio 44135

James E. Anderson
Hana Microdisplay Technologies Inc.
Twinsburg, OH 44087

Philip J. Bos, MEMBER SPIE
Kent State University
Liquid Crystal Institute
Kent, Ohio 44242
E-mail: pbos@kent.edu

Abstract. 2-D optical phased array antennas formed by a liquid crystal on silicon (LCOS) spatial light modulator are described for free-space laser communication and high-resolution wavefront control. The device consists of an 2-D array of 1024×768 phase modulator elements, each with controlled voltage, and can induce a phase shift from 0 to 2π for wavelengths up to the near IR. When the device is used as a wavefront corrector, 18.7 waves peak-valley (at 632.8 nm) of aberration in the optical system is corrected to a residual of 1/9 wave peak-valley, or 1/30 wave rms. The Strehl ratio improved from 0.006 to 0.83 after correction. An additional linear phase ramp was added to the correction phase ramp to simultaneously correct and steer the laser beam. Continuous steering over ±4 mrad in the *X-Y* plane with a steering accuracy higher than 10 μrad has been obtained. The 1-D beam-steering efficiency is 80% at the maximum steering angle of 4 mrad. These results suggest that an LCOS device can be used to achieve very high-resolution wavefront control at very high efficiency.
[DOI: 10.1117/1.1794706]

Subject terms: liquid crystal on silicon (LCOS); spatial light modulator; optical phased array; wavefront control.

Paper 030481 received Sep. 30, 2003; revised manuscript received Nov. 17, 2004; accepted for publication Apr. 29, 2004.

1 Introduction

Liquid-crystal (LC) spatial light modulators have been under investigation recently as a potential candidate for high-resolution wavefront control in active and adaptive optical systems.[1–3] A major reason for this is that the cost of a LC device is several orders of magnitude lower than that of a conventional deformable mirror or microelectromechanical system (MEMS). Yet, as has been made clear by Gruneisen et al.,[4] the real potential of these devices lies in their high resolution of wavefront control, which allows correction for large high-order aberrations in an optical system. This will be critical to the next generation of space-deployable large optics for laser communication; such large corrections are essential for compensating vibration, thermal expansion, and manufacturing imperfections in large, lightweight, space-deployable optics.[4]

The liquid crystal on silicon (LCOS) device described here has 786,000 pixels on a panel with an effective stroke length of 1 wave. Wavefront correction is achieved by putting a correction phase map, which is modulated by 2π, onto the LCOS. The high resolution and small pixel size of the device allow wavefront correction with resets to achieve very high efficiency for high-order aberration on the primary mirror. In principle, our device can correct 1-wave-magnitude aberration over at least 8 pixels without losing much efficiency. On this basis, our device should be capable of correction of tip and tilt up to 125 waves, and primary spherical aberration up to around 50 waves peak to valley (PV) at high efficiency.

A strong diffraction effect can be observed in these devices, as the pixel size is very small; the diffraction efficiency can be low if the phase profile of these devices is aberrated from the ideal for any of a number of reasons.[5–7] One unavoidable limitation on an LC device is that the orientation of the LC cannot change drastically at resets where the phase shift goes from 0 to 2π. This will happen in regions of flyback and lower the diffraction efficiency. In this paper, we provide experimental results on the quality of wavefront compensation and the diffraction efficiency of these devices. Comparisons between the experimental results and numerical simulations of optical propagation are also shown.

2 Device Characterization

The LCOS device is manufactured by Hana Microdisplay and is shown in Fig. 1. The long axis of the device is defined as the *Y* axis, and the short axis as the *X* axis. The specification of the LCOS device is given by Table 1. It is driven by display driver, and the control signal is a certain grayscale image generated by a computer. The driver maps the grayscale image into a voltage signal to each pixel on the LCOS.

The electro-optical (EO) response of the LCOS device is shown in Fig. 2. Instead of direct wavefront measurement, the optical path difference (OPD) between the ordinary and extraordinary rays of light in the LC is measured. The incident polarization of the light is at 45 deg with respect to the fast axis of the LCOS device. This birefringence measurement only measures the OPD due to the LC layer, as only the LC layer will change the OPD difference between ordinary light and extraordinary light. And this measure-

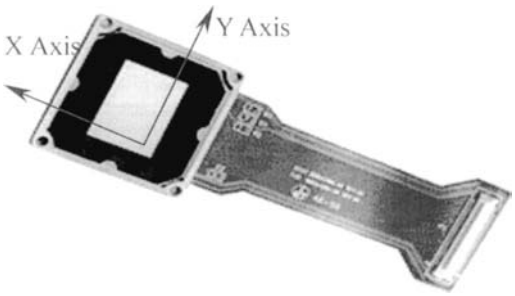

Fig. 1 Hana Microdisplay manufactured LCOS device.

ment is far more accurate than direct wavefront measurement.

The EO curve for both the central part of the device and an array of 100×100 points across the device was measured. The EO curve obtained by measuring the central part of the device is what we called the 1-D measurement, and the 100×100-point measurement is what we called the 2-D measurement. The EO response curve is slightly different on different parts of the device, due to nonuniformity in cell gap, rubbing, etc., as shown in Fig. 3, the birefringence map of the LCOS device at zero voltage. As we can clearly see, the birefringence value at the center of the device is different than that on the edge. Also, for different applied voltages, or different grayscales, the measured birefringence map is not the same.

In Fig. 4, the maximum PV OPD is plotted as a function of grayscale. The nonuniformity for both low and high grayscale is less than λ/20; for the middle range between grayscale 120 and 180, the nonuniformity is apparently higher. At low grayscale, the tilt of the LC director in the bulk is small, so the maximum PV OPD is comparable to that at the zero-voltage stage. At high grayscale, because the LC director is aligned nearly to perpendicular to the surface, LC close to the surface layer contributes the most to the OPD variation. The effective extraordinary refractive index corresponding to that tilt state is close to the ordinary refractive index n_o of the LC material, so the difference between the effective extraordinary refractive index and ordinary refractive index is very small compared with that at the zero-voltage stage. In this case, even for the same amount of orientation variation in the LC director, the maximum OPD will be smaller than at the zero-voltage stage. For grayscales in the middle range, since the director orientation is most sensitive to applied voltage, and the difference between the effective extraordinary refractive index and the ordinary refractive index is still large, the cumulative OPD is more susceptible to nonuniformity (in voltage, cell gap, etc.). As a result, the maximum PV OPD is found to be in this middle grayscale range.

Another observation is that less than 1% depolarization is observed in the middle grayscale range, where the out-of-plane director component is most apparent. This is partially due to the fact that an LC director twist configuration is formed in the cell because of fringe field effect from adjacent activated pixels, which also explains why the maximum PV OPD is largest in the middle voltage range. Nevertheless, the device is very uniform: the maximum OPD variation across the LCOS device is less than λ/12 PV at 632.8 nm for any grayscale.

Table 1 Specification of liquid-crystal-on-silicon spatial light modulator.

Cell type	Visible version	Near-IR version
Active area	20 mm×15 mm	20 mm×15 mm
Fill factor	96%	96%
Resolution	1024×768	1024×768
Bit depth	8-bit 256-grayscale	8-bit 256-grayscale
Temporal bandwidth	50 Hz	5 Hz
Effective stroke length	700 nm (measured at 632.8 nm)	2060 nm (measured at 1550 nm)

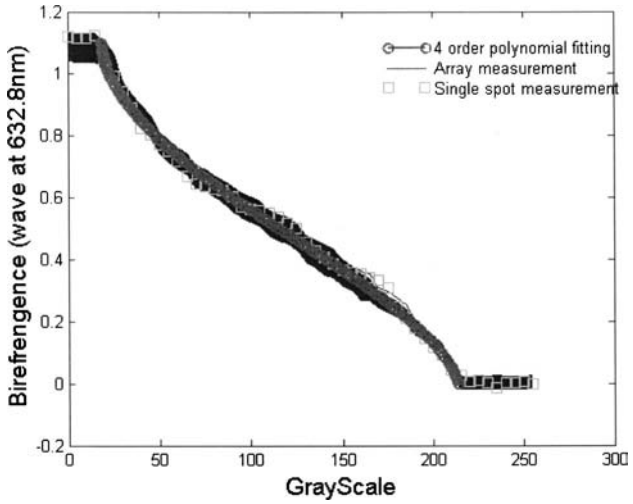

Fig. 2 Electro-optical resoponse of LCOS device: birefringence as function of grayscale.

3 Wavefront Compensation

A Michelson interferometer was used to measure the wavefront of an expanded laser beam reflected from the LCOS

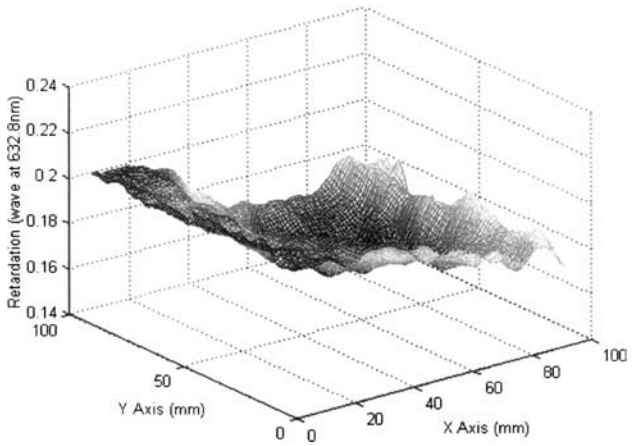

Fig. 3 Nonuniformity across the active area of LCOS device: 2-D birefringence map at zero voltage.

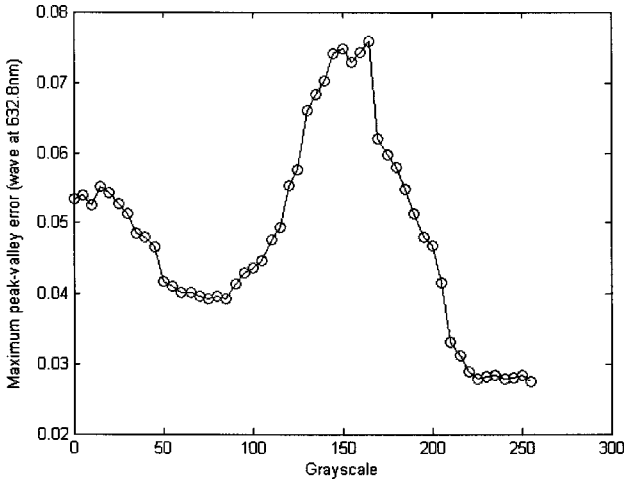

Fig. 4 Nonuniformity of LCOS device for different grayscale: Maximum peak-valley OPD as function of grayscale.

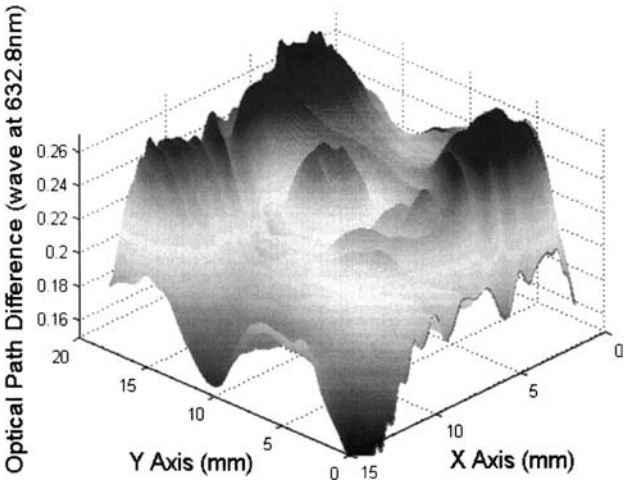

Fig. 6 Measured residual aberration after second compensation.

device. The $1/e^2$ beam waist of the laser was expanded to 9 mm using a spatial filter consisting of a low-aberration microscope objective and a 25-μm-diameter pinhole. A device with a very badly curved substrate was selected to demonstrate our capability of wavefront correction. A seven-step 60-deg shift algorithm[8] was used to reconstruct the phase profile, and phase unwrapping was performed to remove the discontinuity of the phase profile. The obtained wavefront map (Fig. 5) was filtered with a 4×4 Wiener adaptive noise removal filter to reduce high-frequency noise of the phase profile. The aberration to the wavefront is 18.7 waves PV at 632.8 nm, or 3.97 waves rms. By combining the EO curve of the LCOS device and the measured wavefront map, a conjugate compensation image is generated and displayed on the LCOS device. Since the effective stroke length of the device is 1 wave, the aberrated wavefront is modulated by 1 wave in the compensation image. Thus, for every wave of aberration, the phase profile has a reset that may cause some discontinuity and local variation in the wavefront.

When the wavefront correction is turned on, the residual wavefront after a first compensation is measured again, and the residual wavefront is around 0.6 waves PV. The residual wavefront is added to the original wavefront, and a second, more accurate compensation image is generated the same way. After the second compensation, the residual wavefront is measured as 0.11 waves (PV) and 0.032 waves rms at 632.8 nm. The main reason that we need a second compensation to achieve very accurate wavefront compensation is that we have such a large aberration in the system that the wavefront measurements are not very accurate due to the aberration of rays. After the first compensation the residual aberration in the system is small and the measurement of the wavefront is more accurate.

The far-field beam profile is measured by focusing the 9-mm-diameter beam and measuring the intensity profile at the focus with a beam profiler from Photon Inc. When there is no LCOS device in the system, the focused laser beam has a diameter of 107.3 μm, or about 1.11 times the calculated diffraction-limited beam diameter. The optical system without the LCOS device is well corrected and can be regarded as aberration-free. The reflectivity of the aluminum mirror on the silicon backplane is not very high, for no dielectric layer has been applied to enhance the reflectivity, and there is some diffraction loss due to the discontinuity of the aluminum mirror and some loss at the glass surface. As a result, the reflectivity of the LCOS panel, while collecting only the primary diffraction peak, is not very high, 80.4%. In order to separate the effects of reflectivity and wavefront quality on the Strehl ratio, we take the peak intensity of the focused laser beam and reduce that number by 80.4% as the reference. This corresponds in our subsequent discussion to a Strehl ratio of 1.0. The Strehl ratio of the compensated beam versus the noncompensated beam can easily be calculated from the corrected peak intensities. As shown in Fig. 6, the Strehl ratio of the noncompensated beam is 0.006, and that of the compensated beam is 0.83.

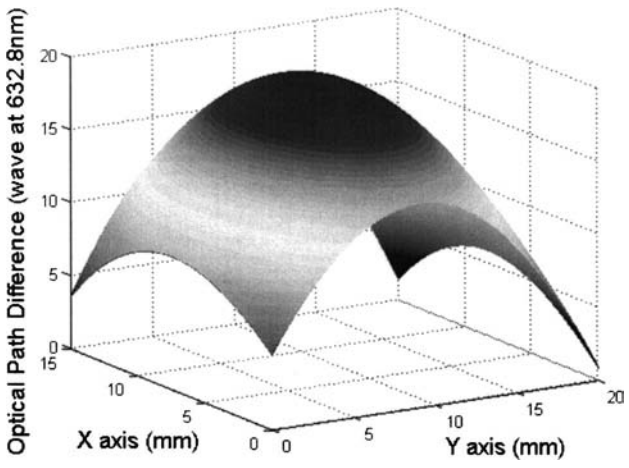

Fig. 5 Measured aberration in the wavefront before compensation.

4 Beam Steering after Compensation

After compensation, an additional linear phase ramp was added to the compensated image to combine compensation with beam steering. The image displayed on the LCOS device now has the dual purpose of compensating for the aberration and beam steering. For a steering-angle range

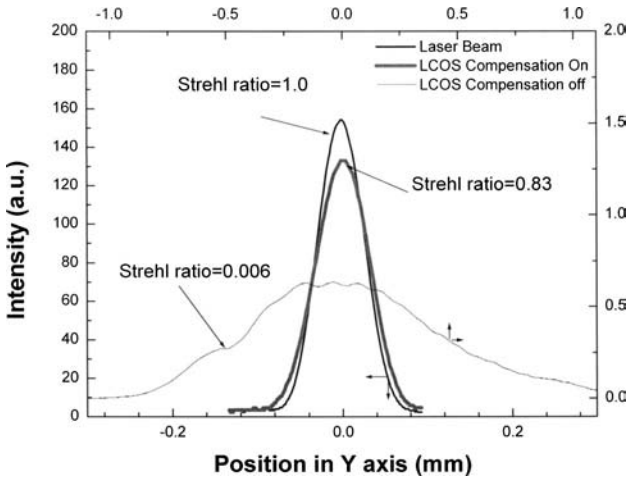

Fig. 7 Beam profile at focus before and after compensation.

$\Delta\theta = 1\ \mu$rad to 4.6 mrad, 36 steering angles were measured, and each steering angle was the same along the X and Y axes: $\Delta\theta = \sqrt{2}\,\Delta\theta_x = \sqrt{2}\,\Delta\theta_y$. Within the designated steering range of ± 4 mrad, the beam remains at very high quality with an ellipticity of less than 4%, a beam waist less than 1.32 times the diffraction-limited beam waist, and a Strehl ratio higher than 0.66. Figure 7 shows the intensity profile at focus for both the steered and nonsteered beams.

Since our wavefront correction is not a continuous one but a stairlike blazed grating, resets split the continuous wavefront and produce some discontinuity in the wavefront. Although the OPD on the two sides of the resets is matched to have only 1 wave of difference, some local perturbation of the wavefront will lower the diffraction efficiency. This is becasue because the director orientation of the LC cannot change drastically, and the phase profile is not ideal, as shown in Fig. 8. This figure shows a calculation of the phase profile with a certain voltage profile added on each pixel. A flyback region of size about half a pixel can be observed from the simulation results.

The diffraction efficiency of an ideal grating with a stairstep blaze is given by[5]

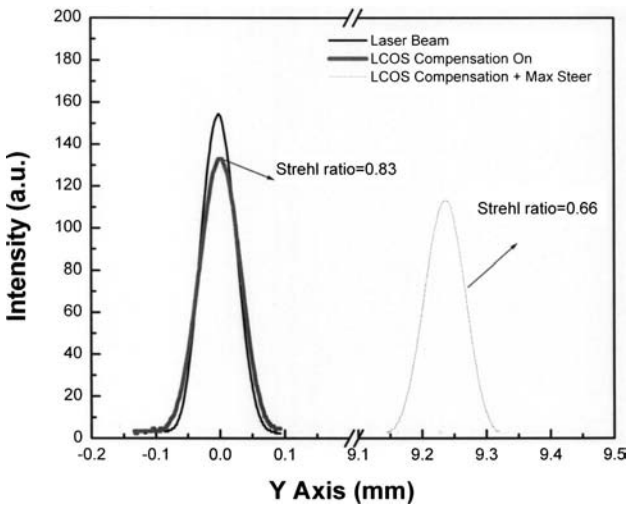

Fig. 8 Beam profile of steered and non-steered beam.

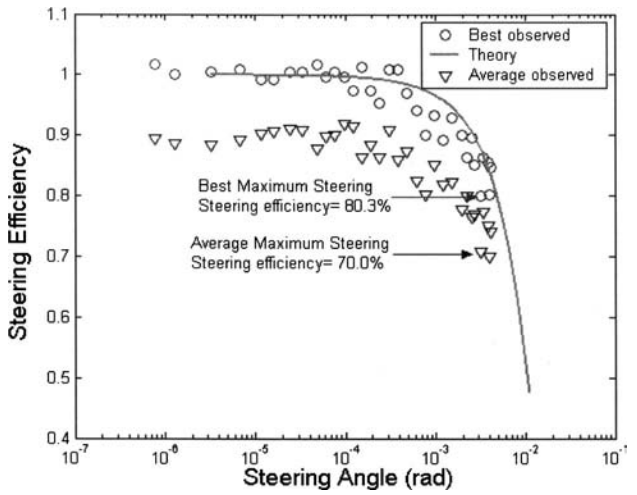

Fig. 9 Steering efficiency as function of steering angle after wavefront compensation.

$$\eta = \left[\frac{\sin(\pi/q)}{\pi/q}\right]^2. \tag{1}$$

Here q is the number of steps in the blaze profile. Any light passing through flyback regions of the device will be diffracted to a nonzero-order peak and should be considered as total loss. An adjustment incorporating this phenomenon can be made in the expression for diffraction efficiency:

$$\eta_{\text{total}} = \left[\frac{\sin(\pi/q)}{\pi/q}\right]^2 \left(1 - \frac{\Lambda_F}{\Lambda}\right)^2. \tag{2}$$

Here Λ_F is the width of the flyback region, and Λ is the total length of that period of the grating. By using the peak intensity of the beam after compensation as a reference, we can define the steering efficiency as the ratio of the peak intensity of the compensated and steered beam to that of the compensated nonsteered beam. Then the steering efficiency as function of steering angle is shown in Fig. 9. The theoretical curve is calculated by assuming that width Λ_F of the flyback region is 0.5 pixel, or about 10 μm. We define the maximum steering angle of our device to be 8 pixels per reset, or 4.0 mrad. If we steer the beam past this angle, the steering efficiency drops drastically. At the maximum steering angle of 4 mrad, the measured steering efficiency is around 80%, which is very close to the theoretical value of 84%. A 2-D finite-difference time-domain (FDTD) calculation has also been carried out, and in the simulated far-field pattern, 86% of the energy goes into the primary diffraction peak.

The beam-steering accuracy has been studied by measuring the average peak position of the focused far-field spot. The accuracy of this position measurement is higher than 0.5 μm. At a distance of 1 m our steering-angle accuracy can be as high as 0.5 μrad, considering only the limitation of position measurement accuracy. However, the pointing stability of our He-Ne laser, vibration, and the airflow in the experimental environment deteriorate the accuracy to around 7 μrad. For the expanded laser beam, the minimum beam waist is 9 mm and the diffraction-limited

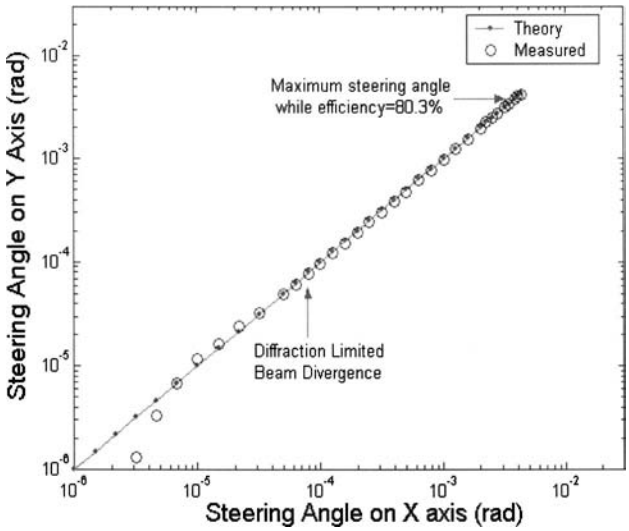

Fig. 10 Steering accuracy of LCOS device.

beam divergence θ can be estimated as $\theta = 1.27 \times \lambda / d = 1.27 \times 0.63/9000 = 89$ μrad. The measured steering accuracy is shown in Fig. 10. Over the whole steering range of ± 4 mrad, the maximum steering error on both *X* and *Y* axes is less than 10 μrad, or about 1/10 of the diffraction-limited beam divergence. The steering accuracy in our measurement is close to the highest accuracy we can possibly achieve in our current environment.

There has been some speculation that these stairlike blazed gratings can only steer the beam to discrete angles with high efficiency, but it has been shown by Titus et al.[9] that continuous steering with high efficiency is possible. Here we have shown continuous steering within ± 4 mrad at high efficiency. For the 36 points measured over the whole steering range, the steering angle is not set to make the number of steps per grating period, *q*, an integer in Eq. (2). Indeed, *q* can be any real number greater than 8 to ensure high efficiency. Thus, we can steer the laser beam continuously within the whole steering range at high efficiency. In those pixels that contain resets, the phase is set to some linearly interpolated value of the phase profile. This introduces some efficiency loss, but as long as there are not too many resets across the device, the loss of efficiency is negligible, as shown in our results.

5 Conclusion

We have demonstrated that a liquid crystal on silicon (LCOS) device can be used as an active optical component to compensate for huge wavefront aberrations and yield diffraction-limited performance. Unlike holographic wavefront compensation,[4] which also has been demonstrated to be able to correct for huge aberrations, our method uses direct wavefront measurement and phase reconstruction. The accuracy and efficiency of the compensation have been demonstrated to be very high. We achieved a total optical efficiency of 0.65 in wavefront compensation and 0.58 in compensation plus maximum steering, if we define the optical efficiency as the reflectivity of the LCOS panel times the final Strehl ratio of the focused beam. We have performed 2-D finite-difference time-domain simulations of the device; these yield excellent agreement between experiment and theory. After the compensation for the aberrated wavefront, additional beam steering within a range of ± 4 mrad in both the *X* and *Y* direction is realized. The steering efficiency is higher than 88% for the whole range, while the steering accuracy is as high as 10 μrad, or 1/10 the diffraction-limited beam divergence in an open-loop system. We found no theoretical limit to the steering accuracy of such an LCOS device. The steered beam quality is very high; the far-field beam waist is less than 1.3 times the diffraction-limited spot size for a compensated and steered beam.

Acknowledgments

This work is supported by the DARPA THOR project for LCOS device development and by NASA for system development. The authors thank Michael Fisch and Vassili Sergan for helpful discussion.

References

1. M. T. Gruneisen and J. M. Wilkes, "Compensated imaging by real-time holography with optically addressed spatial light modulators," in *Spatial Light Modulators*, OSA TOPS Vol. 14, G. Burdge and S. C. Esener, Eds., pp. 220–, Optical Society of America, Washington, DC (1997).
2. G. D. Love, "Wavefront correction of Zernike modes with a liquid-crystal spatial light modulator," *Appl. Opt.* **36**(7), 1517–1524 (1997).
3. D. Dayton, S. Restaino, and J. Gonglewski, "Novel spatial light modulators for active and adaptive optics," *Proc. SPIE* **4124**, 78–88 (2000)
4. M. T. Gruneisen, T. Martinez, D. V. Wick, and J. M. Wilkes, "Holographic compensation of severe dynamic aberrations in membrane-mirror based telescope systems," in *High Resolution Wavefront Control: Methods, Devices, and Applications, Proc. SPIE* **3760**, 142–152 (1999).
5. P. F. McManamon, T. A. Dorschner, D. L. Corkum, L. J. Friedman, D. S. Hobbs, M. Holz, S. Lieberman, H. Q. Nguyen, D. P. Resler, R. C. Sharp, and E. A. Waston, "Optical phased array technology," *Proc. IEEE* **84**(2), 268–298 (1996).
6. L. J. Friedman, D. S. Hobbs, S. Lieberman, D. L. Corkum, H. Q. Nguyen, D. P. Resler, R. C. Sharp, and T. A. Dorschner, "Spatially resolved phase imaging of a programmable liquid-crystal grating," *Appl. Opt.* **35**(31), 6236–6240 (1996).
7. V. G. Dominic, A. J. Carney, and E. A. Watson, "Measurement and modeling of the angular dispersion in liquid crystal broadband beam steering devices," *Opt. Eng.* **35**(12), 3371–3379 (1996).
8. K. Creath, "Choosing a phase-measurement algorithm for measurement of coated LIGO optics," *Laser Interferometer X: Techniques and Analysis Proc. SPIE* **4101**, 47–56 (2000).
9. C. M. Titus, J. Pouch, H. D. Nguyen, F. Miranda, and P. J. Bos, "Diffraction efficiency of thin film holographic beam steering devices," in *High Resolution Wavefront Control: Methods, Devices, and Applications, Proc. SPIE* **4825**, 177–188 (2002).

Xinghua Wang received his BS degree in polymer chemistry from the University of Science and Technology of China in 2000. He is currently pursuing the PhD degree at the Liquid Crystal Institute of Kent State University. His research interest is in liquid-crystal diffractive optical elements, high-resolution wavefront control, laser beam shaping with liquid-crystal spatial light modulator, Optical Phased Array, liquid crystal electro-optical device. He is the former president of Kent State SPIE and current OSA student chapter. He is the student chapter coordinator of Great Lake SPIE Chapter. He serves on organizing committee of liquid crystal technology session of Great Lake Photonic Symposium.

Bin Wang received his BS in physics from Shaanxi Normal University (1984), MS in solid state physics from the Institute of Physics, Chinese Academy of Sciences (1990), and PhD in chemical physics from Kent State University (2002). He currently works as a research associate at the Liquid Crystal Institute, Kent State University. His research interests are applications of liquid-crystal materials, computer simulations for multidimensional liquid-crystal director fields, and optical calculations.

John Pouch received a PhD degree in physics, with a minor degree in mathematics, from Wayne State University, Detroit, MI, in 1981. Since 1983, he has been employed at NASA's John H. Glenn Research Center in Cleveland, Ohio. He is a member of the Antenna, Microwave and Optical Systems Branch. His current activities include managing projects which deal with new optical communications technologies. These efforts are being carried out by academia and industry. He has co-authored over 55 papers in scientific journals and proceedings volumes, and over 75 presentations at national and international conferences. He has also co-edited five books (13 volumes) and two conference proceedings volumes.

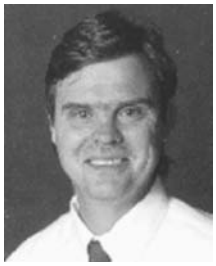

Philip J. Bos received his PhD degree in Physics from Kent State University in 1978. After one year as a research fellow at the Liquid Crystal Institute at Kent State he joined Tektronix Laboratories in the Display Research Department. In 1994 he returned to the Liquid Crystal Institute where he is currently an associate director and a professor of chemical physics. He currently has several projects in the area of applications of liquid crystals. He has over 100 publications and 20 patents.

James Anderson earned his PhD in chemical physics from the Liquid Crystal Institute at Kent State University in 2000. He has written numerous papers on the study of liquid crystals. He has been a member of chaired paper selection committees for several conferences. He is currently Lead Scientist at Hana Microdisplay Technologies.